ON BOARD UNIT DESIGN FOR TRAIN POSITIONING BY GNSS

Alessandro Neri[1], Cosimo Stallo[2], Andrea Coluccia[2], Veronica Palma,[1]Marina Ruggieri[2], Fabrizio Toni[1], Pietro Salvatori[1] Francesco Rispoli[3]

[1]Radiolabs Consortium, Via Arrigo Cavalieri 26, Rome, Italy
e-mail: alessandro.neri@radiolabs.it
[2]Electronic Engineering Department, "Roma Tor Vergata" University, Italy
e-mail: ruggieri@uniroma2.it
[3]Ansaldo STS, Genoa, Italy
e-mail: francesco.rispoli@ansaldo-sts.com

ABSTRACT

The paper shows the architecture of a Location Determination System based on GNSS (GNSS-LDS), mainly focusing on the design of on Board Unit (OBU) installed on a train.
The work is inserted in the scenario of introduction and application of space technologies based on the ERTMS (European Railways Train Management System) architecture, bundling the EGNOS-Galileo infrastructures in the train control system. It aims at improving performance, enhancing safety and reducing the investments on the railways circuitry and its maintenance.
The algorithm core for determining the train location will be showed together with results of a campaign test acquired on a important highway (GRA: Grande Raccordo Anulare) around Rome (Italy) to simulate train movement on a generic track.

***Index Terms*—** Position, Velocity and Time (PVT), Global Positioning System (GPS), Signal In Space (SIS) Integrity, Train Control, Weighted Least Square(WLS) and Railway Safety.

1. INTRODUCTION

Satellite positioning and hybrid (satellite-terrestrial) Telecommunication networks are assumed to replace the traditional means which are part of the ERTMS (European Railways Train Management System) architecture in order to reduce the investments on the railways circuitry and its maintenance. These solutions will be applied to the local and regional lines and low traffic lines that represent all together about 50% of the railway length in Europe [1].
The paper will outline the architecture of a GNSS LDS including the augmentation network compliant with the highest safety level required by the railways norms (SIL-4). A special focus will be dedicated to the OBU algorithm for PVT estimation.
The paper is organized as follows. Section 2 introduces an overview of the GNSS-LDS architecture. Section 3 shows the OBU PVT Estimation algorithm on railway tracks. Section 4 describes the results of a campaign test acquired by a car on GRA. Finally, Section 5 presents our conclusions.

2. GNSS-LDS ARCHITECTURE

The system includes the design, implementation and deployment of a Location Determination System based on GNSS composed of:

a. an Augmentation and Integrity Monitoring Network (AIMN subsystem) further decomposed in:
   a) a set of Reference Stations (RS), with Range and Integration Monitoring capabilities, deployed along the railway track;
   b) a data processing center where the Track Area LDS Server (TALS) – a dedicated resource for the evaluation of augmentation and integrity information – is located. TALS jointly processes the Ranging & Integrity Monitoring (RIM) data and produces the augmentation data feed to the On Board units;
b. an OBU subsystem installed on the train, which feeds the existing Automatic Train Protection system with PVT estimates and/or the "virtual balises" based on these estimates.

The AIMN subsystem provides information on SIS integrity to detect and exclude faulty satellites and the differential corrections to be applied by the GNSS LDS OBU. They are needed for compensating for the effects produced by satellite ephemerides and clock offset errors and variation in the propagation delay introduced by ionosphere and troposphere [2].

The GNSS LDS OBU will provide the PVT estimate and confidence interval to the existing localization system and ATP.

Each GNSS LDS OBU is equipped with:

- one or more GNSS receiver(s);
- a local processor performing the PVT estimation starting from local measures, the Track DB and augmentation data received from the TALS server;
- a track database (Track DB).

To guarantee enough growing capability with respect to integrity and availability requirements, the GNSS LDS OBU architectural design supports the deployment of configurations making use of:

- multiple GNSS antennas for increased availability and /or multipath mitigation, each characterised by its own phase center and radiation diagram;
- two or more different GNSS receivers developed by separate manufacturers to avoid common modes of failure;
- multiple independent processing chains;
- a complementary set of integrity mechanisms (e.g. self check).

Figure 1 shows the GNSS-LDS architecture.

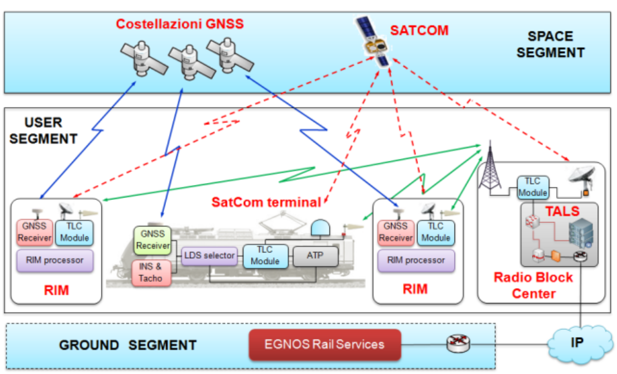

Fig. 1 GNSS-LDS Architecture

3. OBU PVT ESTIMATION

The algorithm for determining the train location explicitly accounts for the fact that the train location is constrained to lie on railway track [3].

In principle, exploiting this constraint allows to estimate train location even when only two satellites are in view. Effective reduction in the number of required satellites to make a fix when track constraint is applied depends on track-satellite geometry. In essence satellites aligned along the track give more information than those at the cross-over. Satellites in excess can then be employed either to increase accuracy or to increase integrity and availability.

For sake of clarity, the PVT estimation algorithm is first illustrated for the case of single GNSS receiver, but, it can be extended to multiple receivers.

From a mathematical point of view, track constraint can be imposed by observing that the train location at a given time *t* is completely determined by the knowledge of its distance from one head end, i.e., by the curvilinear abscissas defined on the georeferenced railway track.

Let *s(t)* be the curvilinear abscissa of a train reference point, like the centre of the antenna of the GNSS receiver, when the GNSS pseudoranges at time are *t* measured. Without loss of generality, we refer here the train reference point to a local frame, i. e. to a frame whose first axis is oriented to Est, the second to North, and the third along the local vertical, pointing up.

Thus subscripts E, N, U will identify the corresponding coordinates. Incidentally we observe that since we are measuring ranges (or pseudo-ranges) and the Euclidean L2 norm is invariant with respect to changes of orthonormal basis, the measurement equations can be equivalently expressed in any orthonormal basis. Nevertheless, using the (Est, North, Up) frame simplifies the application of the track constraint in the subsequent location evaluation iterative procedure.

Then, observing that the Cartesian coordinates with respect to a local (Est, North, Up) of that point are described by the parametric equations:

$$\begin{aligned} X^{Train}(t) &= X^{Train}\{s(t)\} = \\ &= \left[x_E^{Train}[s(t)] \quad x_N^{Train}[s(t)] \quad x_U^{Train}[s(t)]\right]^T \end{aligned} \qquad (1)$$

the pseudoranges measured by the GNSS receiver can be directly expressed in terms of the unknown curvilinear abscissa. In fact, the pseudo-range $\rho_i(k)$ of the *i-th* satellite measured by the OBU GNSS receiver can be written as follows:

$$\begin{aligned} \rho_i(k) &= \left\| X_i^{Sat}\left[T_i^{Sat}(k)\right] - X^{Train}\left[s\left(T_i^{Train}(k)\right)\right] \right\| + \\ &+ c\Delta\tau_i^{ion}(k) + c\Delta\tau_i^{trop}(k) + c\delta t^{Train}(k) \\ &+ n_i^{Train}(k) - c\delta t_i^{Sat}(k) \end{aligned} \qquad (2)$$

where:

$T_i^{Sat}(k)$ is the time instant on which the signal of the *k-th* epoch is transmitted from the *i-th* satellite;

$X_i^{Sat}\left[T_i^{Sat}(k)\right]$ is the coordinate vector of the *i-th* satellite at time $T_i^{Sat}(k)$;

$\Delta\tau_i^{ion}(k)$ is the ionospheric incremental delay along the path from the *i-th* satellite to the GNSS receiver for the k-th epoch w.r.t. the neutral atmosphere;

$\Delta\tau_i^{trop}(k)$ is the tropospheric incremental delay along the path from the *i-th* satellite to the GNSS receiver for the k-th epoch w.r.t. the neutral atmosphere;

δt_i^{Sat} is the offset of the *i-th* satellite clock for the *k-th* epoch;

$T_i^{Train}(k)$ is the time instant of reception by the OBU GNSS receiver of the signal of the *k-th* epoch transmitted by the *i-th* satellite;

$\delta t^{Train}(k)$ is the OBU receiver clock offset;

$n_i^{Train}(k)$ is the error of the time of arrival estimation algorithm generated by multipath, GNSS receiver thermal noise and eventual radio frequency interference.

For sake of compactness in the following we drop temporal dependence on the epoch index. Incidentally we observe that if the sphere centered at a given satellite with radius equal to the measured pseudorange does not intersect the track, or intersect the track in more than one place. It simply means that the information carried by that satellite is ambiguous and the localization problem has to be solved by adding more satellites.

In principle, the same situation may arise in conventional (unconstrained) GNSS localization if the train location and the satellites are near colinear. More frequently, ambiguity appears when dealing with carrier phase tracking.

Let:

$\hat{X}_i^{Sat}\left[T_i^{Sat}\right]$ be the coordinate vector of the *i-th* satellite estimated on the basis of the broadcasted navigation data (and eventual SBAS data where available),

$\Delta\hat{\rho}_i^{Sat}\left[T_i^{Sat}\right]$ be the component of the differential correction related to the ephemerides error of the *i-th* satellite provided by the TALS server (although TALS server provides an overall correction, it can always be modeled as the sum of individual corrections),

$\varepsilon_{\Delta\hat{\rho}_i^{Sat}}\left[T_i^{Sat}\right]$ be the residual estimation error of the differential corrections of the ephemerides error of the *i-th* satellite provided by the TALS server,

so that we can write:

$$\begin{aligned}&\left\|X_i^{Sat}\left[T_i^{Sat}(k)\right]-X^{Train}\left[s\left(T_i^{Train}(k)\right)\right]\right\|=\\&=\left\|\hat{X}_i^{Sat}\left[T_i^{Sat}(k)\right]-X^{Train}\left[s\left(T_i^{Train}(k)\right)\right]\right\|+\\&+\Delta\hat{\rho}_i^{Sat}\left[T_i^{Sat}\right]+\varepsilon_{\Delta\hat{\rho}_i^{Sat}}\left[T_i^{Sat}\right]\end{aligned} \quad (3)$$

In addition let:

$\Delta\hat{\tau}_i^{ion}(k)$ be the component of the differential correction related to estimated ionospheric incremental delay along the path from the *i-th* satellite to the GNSS receiver for the *k-th* epoch w.r.t. the neutral atmosphere;

$\Delta\hat{\tau}_i^{trop}(k)$ be the component of the differential correction related to estimated tropospheric incremental delay along the path from the *i-th* satellite to the GNSS receiver for the *k-th* epoch w.r.t. the neutral atmosphere;

$\varepsilon_{\hat{\tau}_i^{ion}}$ be the estimation error of the ionospheric incremental delay along the path from the *i-th* satellite to the GNSS receiver for the *k-th* epoch w.r.t. the neutral atmosphere;

$\varepsilon_{\hat{\tau}_i^{trop}}$ be the estimation error of the tropospheric incremental delay along the path from the *i-th* satellite to the GNSS receiver for the *k-th* epoch w.r.t. the neutral atmosphere;

$n_i^{Train}(k)$ be the measurement error of the OBU GNSS receiver for the *k-th* epoch:

$$n_i^{Train}(k)=n_i^{Train,Mp}(k)+n_i^{Train,Rx}(k)+n_i^{Train,RFI} \quad (4)$$

where:

$n_i^{Train,Mp}(k)$ is the measurement error due to multipath from the *i-th* satellite to the GNSS receiver for the *k-th* epoch;

$n_i^{Train,Rx}(k)$ is the measurement error due to the thermal plus the internal receiver noise affecting the signal received from the *i-th* satellite for the *k-th* epoch;

$n_i^{Train,RFI}$ is the measurement error due to the radio frequency interference affecting the signal received from the *i-th* satellite for the *k-th* epoch;

$\delta\hat{t}_i^{Sat}$ be the component of the differential correction related to estimated offset of the *i-th* satellite clock provided by the TALS server;

$\varepsilon_{\delta\hat{t}_i^{Sat}}$ be estimation error of the offset of the *i-th* satellite clock for the *k-th* epoch, so that we can write $\delta t_i^{Sat}=\delta\hat{t}_i^{Sat}+\varepsilon_{\delta\hat{t}_i^{Sat}}$.

Therefore for *i-th* pseudorange we have:

$$\begin{aligned}\rho_i(k)&=\left\|\hat{X}_i^{Sat}\left[T_i^{Sat}\right]-X^{Train}\left[s\left(T_i^{Train}\right)\right]\right\|+\\&+\Delta\hat{\rho}_i^{Sat}\left[T_i^{Sat}\right]+c\varepsilon_{\Delta\hat{\rho}_i^{Sat}}\left[T_i^{Sat}\right]+c\Delta\hat{\tau}_i^{ion}+\\&+c\Delta\hat{\tau}_i^{trop}-c\delta\hat{t}_i^{Sat}+c\delta t^{Train}+c\varepsilon_{\Delta\hat{\tau}_i^{ion}}+\\&+c\varepsilon_{\Delta\hat{\tau}_i^{trop}}-c\varepsilon_{\delta\hat{t}_i^{Sat}}+n_i^{Train}\end{aligned} \quad (5)$$

Thus, denoting with:

$$\delta\hat{\rho}_i^{Diff}=\Delta\hat{\rho}_i^{Sat}+c\Delta\hat{\tau}_i^{ion}+c\Delta\hat{\tau}_i^{trop}-c\delta\hat{t}_i^{Sat} \quad (6)$$

the overall differential correction provided by the TALS, we finally obtain:

$$\begin{aligned}\rho_i-\delta\hat{\rho}_i^{Diff}&=\rho\left\|\hat{X}_i^{Sat}\left[T_i^{Sat}\right]-X^{Train}\left[s\left(T_i^{Train}\right)\right]\right\|+\\&+c\delta t^{Train}+n_i\end{aligned} \quad \mathbf{(7)}$$

with $n_i=c\varepsilon_{\Delta\hat{\rho}_i^{Sat}}+c\varepsilon_{\Delta\hat{\tau}_i^{ion}}+c\varepsilon_{\Delta\hat{\tau}_i^{trop}}-c\varepsilon_{\delta\hat{t}_i^{Sat}}+n_i^{Train}$ (8)

The pseudo-range equation system can be solved by an iterative procedure based on the first order Taylor's series expansion around a train curvilinear abscissa estimate $\hat{s}^{(m)}$. The initial estimate of the curvilinear abscissa is obtained by first computing the receiver location without track constraint and selecting as initial point for the iteration the nearest track point.

Let us denote with $\tilde{\rho}_i(m)$ the *i-th* pseudorange:

$$\tilde{\rho}_i(m) = \left\| \hat{X}_i^{Sat}\left[T_i^{Sat}\right] - X^{Train}\left[\hat{s}^{(m)}\right] \right\| \quad (9)$$

so that:

$$\begin{aligned} &\rho_i - \delta\hat{\rho}_i^{Diff} - \tilde{\rho}_i^{(m)} - c\delta t^{Train} - n_i = \\ &= \left\| \hat{X}_i^{Sat}\left[T_i^{Sat}\right] - X^{Train}\left[s\left(T_i^{Train}\right)\right] \right\| + \\ &- \left\| \hat{X}_i^{Sat}\left[T_i^{Sat}\right] - X^{Train}\left[\hat{s}^{(m)}\right] \right\| \end{aligned} \quad (10)$$

Then denoting with:

$$\Delta s^{(m)} = s\left(T_i^{Train}\right) - \hat{s}^{(m)} \quad (11)$$

We expand $\left\| \hat{X}_i^{Sat}\left[T_i^{Sat}\right] - X^{Train}\left[s\left(T_i^{Train}\right)\right] \right\|$ in Taylor's series w.r.t.s with initial point $\hat{s}^{(m)}$ then obtaining:

$$\begin{aligned} &\left\| \hat{X}_i^{Sat}\left[T_i^{Sat}\right] - X^{Train}\left[s\left(T_i^{Train}\right)\right] \right\| = \\ &= \left\| \hat{X}_i^{Sat}\left[T_i^{Sat}\right] - X^{Train}\left[\hat{s}^{(m)}\right] \right\| + \\ &+ \left[\frac{\partial\rho_i}{\partial x_E^{Train}} \frac{\partial x_E^{Train}}{\partial s} + \frac{\partial\rho_i}{\partial x_N^{Train}} \frac{\partial x_N^{Train}}{\partial s} + \frac{\partial\rho_i}{\partial x_U^{Train}} \frac{\partial x_U^{Train}}{\partial s} \right]_{s=\hat{s}^{(m)}} \Delta s^{(m)} + n_i^{Taylor} \end{aligned} \quad (12)$$

where n_i^{Taylor} accounts for the expansion truncation.

Then, we finally obtain:

$$\begin{aligned} &\rho_i - \delta\hat{\rho}_i^{Diff} - \tilde{\rho}_i^{(m)} = \\ &= \left[\frac{\partial\rho_i}{\partial x_E^{Train}} \frac{\partial x_E^{Train}}{\partial s} + \frac{\partial\rho_i}{\partial x_N^{Train}} \frac{\partial x_N^{Train}}{\partial s} + \frac{\partial\rho_i}{\partial x_U^{Train}} \frac{\partial x_U^{Train}}{\partial s} \right]_{s=\hat{s}^{(m)}} \Delta s^{(m)} + \\ &+ c\partial t^{Train} + n_i + n_i^{Taylor}, \quad i = 1,\ldots,N_{Sat} \end{aligned} \quad (13)$$

where N_{Sat} is the number of visible satellites.

Then, denoting with $\Delta\rho_i^{(m)}$ the differential reduced pseudorange at the *m-th* iteration:

$$\Delta\rho_i^{(m)} = \rho_i - \delta\hat{\rho}_i^{Diff} - \tilde{\rho}_i^{m} \quad (14)$$

the corresponding N_{Sat} scalar linear equations can be written in compact matrix notation as follows:

$$\Delta\boldsymbol{\rho}^{(m)} = \mathbf{H}^{(m)}\mathbf{D}^{(m)}\mathbf{z} + \boldsymbol{\nu} \quad (15)$$

where:

$$z = \begin{bmatrix} \Delta s^{(m)} \\ c\delta\delta^{Train} \end{bmatrix} \quad (16)$$

D is the matrix with elements given by the directional cosines of the tangent to the railway track at time *t*:

$$\mathbf{D}^{(m)} = \begin{bmatrix} \left[\frac{\partial x_E^{Train}}{\partial s}\right]_{s=\hat{s}^{(m)}} & 0 \\ \left[\frac{\partial x_N^{Train}}{\partial s}\right]_{s=\hat{s}^{(m)}} & 0 \\ \left[\frac{\partial x_U^{Train}}{\partial s}\right]_{s=\hat{s}^{(m)}} & 1 \\ 0 & 1 \end{bmatrix}, \quad (17)$$

H is the classical N_{Sat}x4 observation matrix:

$$\mathbf{H}^{(m)} = \begin{bmatrix} \mathbf{P}^{(m)} & \mathbf{1}_{N_{Sat}} \end{bmatrix} \quad (18)$$

where **P** is the N_{Sat}x3 Jacobian matrix of the pseudo-ranges with respect to the Cartesian train coordinates,

$$\mathbf{P}^{(m)} = \left[\frac{\partial\tilde{\rho}^{(m)}}{\partial X^{Train}}\right]_{X^{Train}=X^{Train}\left[\hat{s}^{(m)}\right]} =$$

$$= \begin{bmatrix} \left[\frac{\partial\tilde{\rho}_1^{(m)}}{\partial x_E^{Train}}\right]_{X^{Train}=X^{Train}\left[\hat{s}^{(m)}\right]} & \left[\frac{\partial\tilde{\rho}_1^{(m)}}{\partial x_N^{Train}}\right]_{X^{Train}=X^{Train}\left[\hat{s}^{(m)}\right]} & \left[\frac{\partial\tilde{\rho}_1^{(m)}}{\partial x_U^{Train}}\right]_{X^{Train}=X^{Train}\left[\hat{s}^{(m)}\right]} \\ \left[\frac{\partial\tilde{\rho}_2^{(m)}}{\partial x_E^{Train}}\right]_{X^{Train}=X^{Train}\left[\hat{s}^{(m)}\right]} & \left[\frac{\partial\tilde{\rho}_2^{(m)}}{\partial x_N^{Train}}\right]_{X^{Train}=X^{Train}\left[\hat{s}^{(m)}\right]} & \left[\frac{\partial\tilde{\rho}_2^{(m)}}{\partial x_U^{Train}}\right]_{X^{Train}=X^{Train}\left[\hat{s}^{(m)}\right]} \\ \left[\frac{\partial\tilde{\rho}_{N_{Sat}}^{(m)}}{\partial x_E^{Train}}\right]_{X^{Train}=X^{Train}\left[\hat{s}^{(m)}\right]} & \left[\frac{\partial\tilde{\rho}_{N_{Sat}}^{(m)}}{\partial x_N^{Train}}\right]_{X^{Train}=X^{Train}\left[\hat{s}^{(m)}\right]} & \left[\frac{\partial\tilde{\rho}_{N_{Sat}}^{(m)}}{\partial x_U^{Train}}\right]_{X^{Train}=X^{Train}\left[\hat{s}^{(m)}\right]} \end{bmatrix} \quad (19)$$

with elements given by the directional cosines of the satellite lines of sight:

$$P_{ij}^{(m)} = \left[\frac{\partial\tilde{\rho}_i^{(m)}}{\partial x_j^{Train}}\right]_{X^{Train}=X^{Train}\left[\hat{s}^{(m)}\right]} = -\frac{\hat{x}_{i,j}^{Sat} - x_j^{Train}\left(\hat{s}^{(m)}\right)}{\left\|X_i^{Sat} - X^{Train}\left(\hat{s}^{(m)}\right)\right\|}, j = E, N, U \quad (20)$$

and $1_{\mathbf{N_{Sat}}}$ is the N_{Sat}x1 vector:

$$1_{N_{Sat}} = \begin{bmatrix} 1 \\ 1 \\ \vdots \\ 1 \end{bmatrix} \quad (21)$$

and

$$\begin{aligned} &\nu_i = n_i + n_i^{Taylor} = c\varepsilon_{\Delta\hat{\rho}_i^{Sat}} + c\varepsilon_{\Delta\hat{\tau}_i^{ion}} + c\varepsilon_{\Delta\hat{\tau}_i^{trop}} - c\varepsilon_{\delta\hat{t}_i^{Sat}} \\ &+ n_i^{Train} + n_i^{Taylor}, \quad i = 1,2,..N_{Sat} \end{aligned} \quad (22)$$

represents the equivalent observation noise.

The set of linear equations (15) may be solved w.r.t. the curvilinear abscissa and the receiver clock offset by means of a WLS method. In principle, extended Kalman filter algorithms could also be considered, and then accounting for train dynamics. Since use of memoryless location determination algorithms is a major requirement, the WLS algorithm, that implements by fact only the static part of the Kalman filter equations, has been considered as a candidate solution.

Therefore, the described algorithm can be directly employed when a mix of satellites from different constellations are used, as far as eventual differences in their timing references are pre-compensated.

Nevertheless it can be also applied to subsets of the visible satellites belonging to the same constellation.

Recently, particle filters have been proposed in place of extended Kalman filters to solve the pseudorange nonlinear equations. Nevertheless, their computational complexity qualifies them as not mature for high integrity receivers [3].

At each iteration, the WLS estimate $\hat{\mathbf{z}}$ is computed as:

$$\hat{\mathbf{z}}^{(m+1)} = \mathbf{K}^{(m)}\Delta\boldsymbol{\rho}^{(m)}, \quad (23)$$

where $\mathbf{K}^{(m)}$ is the gain matrix:

$$\mathbf{K}^{(m)} = \left(\left[\mathbf{D}^{(m)}\right]^T\left[\mathbf{H}^{(m)}\right]^T\mathbf{R}_\nu^{-1}\mathbf{H}^{(m)}\mathbf{D}^{(m)}\right)^{-1}\left[\mathbf{D}^{(m)}\right]^T\left[\mathbf{H}^{(m)}\right]^T\mathbf{R}_\nu^{-1} \quad (24)$$

In addition, the variance of the estimate of the curvilinear abscissa *s* computes as follows:

$$\sigma_s^2 = \left[R_{\Delta\hat{z}}\right]_{1,1} = \left[\left(\left[D^{(m)}\right]^T \left[H^{(m)}\right]^T R_\upsilon^{-1} H^{(m)} D^{(m)}\right)^{-1}\right]_{1,1} \quad (25)$$

Velocity is estimated on the basis of Doppler speed measurements coming from the external GNSS receivers. Acceleration is estimated on the basis of the estimated velocity history.

Computation of the standard deviation of the estimation errors will account for actual satellite line of sights, nominal values of the receiver noise and multipath, standard deviations of the user equivalent differential range error provided by the TALS server.

4. RESULTS

This section is devoted to show the main algorithm results based on comparison of its output with campaign of measurements based on the processing, in Matlab environment, of the results of a measurement campaign acquired by a car along the GRA highway in the city of Rome (Italy).

Two RIMs are located along the GRA and used for generating the corrections to be sent to the OBU.

Both RIMs are equipped with two receivers (nvs and u-blox) and a car, acting as OBU, is moving along the highway and it is equipped with the same receivers.

In Figures 2 and 3, PVT estimation and its statistics are depicted.

In detail, in Figure 2, the position estimate versus the ground truth is depicted and it is possible to notice that the error is included in a range of ±2.6 meters.

In Figure 3, it is possible to notice the deviation standard of the position estimate is bounded between [0.8, 2.3] meters. Finally, in Figure 4, the velocity estimation is represented.

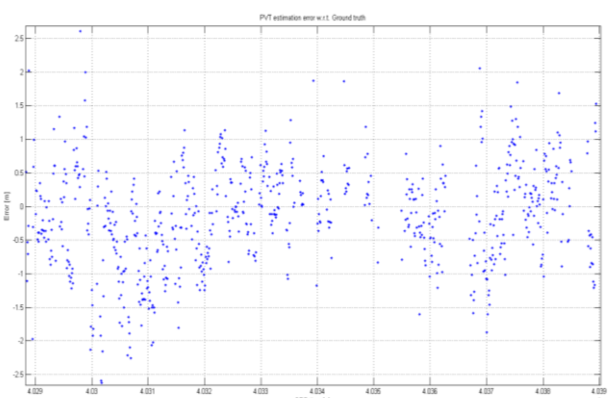

Fig. 2: Estimated PVT Error & Ground Truth versus GPS Time

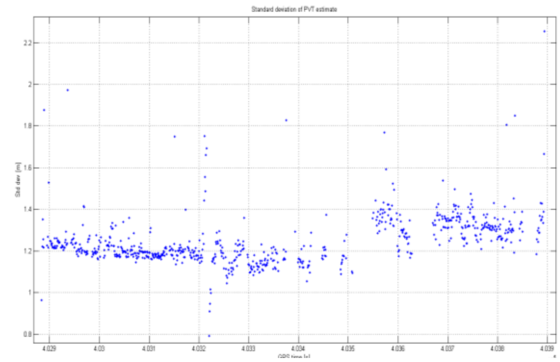

Fig. 3: Estimated PVT Standard Deviation versus GPS Time

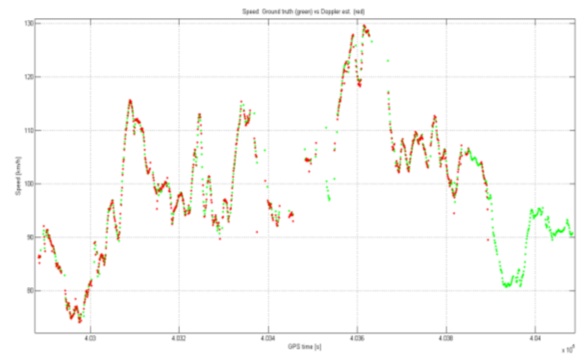

Fig. 4: Estimated Train Speed based on Doppler Shift (red) & Ground Truth (green) versus GPS Time

5. CONCLUSIONS

The paper shows the architecture of a GNSS-LDS, focusing on the design of OBU installed on train. The work is inserted in the scenario of introduction and application of space technologies based on the ERTMS architecture to improve performance and enhance safety, reducing the investments on the railways circuitry and its maintenance. The algorithm core for determining the train location is described comparing its results with data acquired by car along the GRA highway.

6. REFERENCES

[1] A. Basili, et al. "A Roadmap for the adoption of space assets for train control systems: The Test Site in Sardinia", IEEE ESTEL Conference, Rome, 2-5 October 2012.

[2] R.E Phelts, et al. "Characterizing Nominal Analog Signal Deformation on GNSS Signals" , ION GNSS 2009, Savannah, GA, September 2009, pp. 1343-1350.

[3] A. Neri, et al. "An Analytical Evaluation for Hazardous Failure Rate in a Satellite-based Train Positioning System with reference to the ERTMS Train Control Systems", ION GNSS 2012, Nashville, TN, September 2012.